



PHASE-FIELD STUDY OF RAPID DIRECTIONAL SOLIDIFICATION IN A HIGHLY SUPERCOOLED MELT

Mauricio Fabbri

fabbri@saofrancisco.edu.br

Unidade Acadêmica da Área de Ciências Exatas e Tecnológicas – UAACT

Universidade São Francisco

Rua Alexandre Rodrigues Barbosa, 45, 13.251-900, Itatiba - SP – Brazil

Abstract. *We describe a simple numerical procedure to investigate the solid-liquid interface kinetics by Phase Field (PF) techniques. The main idea is to consider a one-dimensional slab of melted material that is kept highly undercooled by a strong coupling to a heat sink; distinct regimes of phase-change can then be studied by varying the Biot number Bi . In that manner, the form factor of the PF kinetic parameter is obtained by linear regression, using the numerical results for the interface speed versus local temperature, in the regime $Bi \rightarrow \infty$. The diffuse interface PF model is also compared and validated with respect to classical sharp-interface results.*

Keywords: *Phase Field methods, Rapid Solidification, Stefan problems*

1. INTRODUCTION

Computer simulation of solidification processes far away from equilibrium is a challenge for classical models. For a pure substance, engineering studies are usually based on the assumption that the phase state is a unique function of temperature, thus requiring explicit kinetic corrections and somewhat involved schemes to cope with metastable regimes. Those drawbacks can be overcome *ab-initio*, by the use of a suitable thermodynamic functional which correctly describes the energetics which favors solidification, thus allowing undercooled (metastable) states as natural possible solutions. The phase-field (PF) methods, which appeared in the last two decades, are nowadays among the best alternatives to classical techniques – they not only include a correct thermodynamic description of phase-change processes, but also avoid the explicit tracking of the moving interface (Caginalp, 1980; Warren, 1995). PF algorithms are capable of encompassing virtually any form of anisotropy and interface kinetics, and for that reason are currently employed, e.g., for computer simulation of 3D dendritic growth (Karma and Rappel, 1996a) and constitutional instability during alloy solidification (Braun, McFadden and Coriell, 1994; Lan, Shih and Hsu, 2004).

In this work, we develop and implement a simple PF algorithm to investigate the interface speed and local temperature during rapid directional solidification. The main concern being kinetic effects, we consider a one-dimensional heat transfer problem between an uniform heat sink and a slab of a pure substance, which undergoes a liquid-solid phase change. Heat transport is only by conduction inside the material (we neglect convective effects for fast solidification), and the coupling with the heat sink is accounted for by the value of the Biot number (Bi). The regime $Bi \gg 1$ ensures that the melt is maintained highly supercooled at all times; a fraction of the latent heat released at the interface warms the liquid ahead, but the temperature of the melt can be mainly imposed by a high thermal coupling with the surroundings.

Kinetic effects are implicitly handled by PF models, and can be adjusted by an adequate form of the potential and/or by the time relaxation exponent (Fabbri and Voller, 1995; Fazenda, Travelho and Fabbri, 1996). Asymptotic analysis (Karma and Rappl, 1996) shows that PF models with linear time relaxation always imply linear interface kinetics for low local undercoolings. We here describe a simple procedure to match the PF kinetic parameters to the actual known material properties.

The paper is organized as follows. First we review briefly the PF basics and establish the notation and our specific choices; we also describe a simple "travelling-wave" small expansion around the interface region that explains the common linear kinetic behavior of the PF equations. Then, the correct "sharp interface limit" is numerically verified for a well-known classical problem for supercooled solidification (the *benchmark*). We next implement a PF model with a Biot-source type term, describe a calibration procedure which conforms to the asymptotic analysis, and give results about the computed interface kinetics for a range of Bi values.

2. THE PHASE-FIELD EQUATIONS AND ASYMPTOTICS

2.1 Phase equation and potential

PF models introduce a phase variable $p(x,t)$, the values of which describe the phase state of the material on position x at time t . We choose the value $+1$ corresponding to liquid, and -1 to solid. The solid-liquid (S-L) interface is defined by points at which $p=0$. In practice, there is always a transition layer of width ε between the solid and liquid phases (Fig. 1), which can be made as small as desired, in order to approximate a sharp interface.

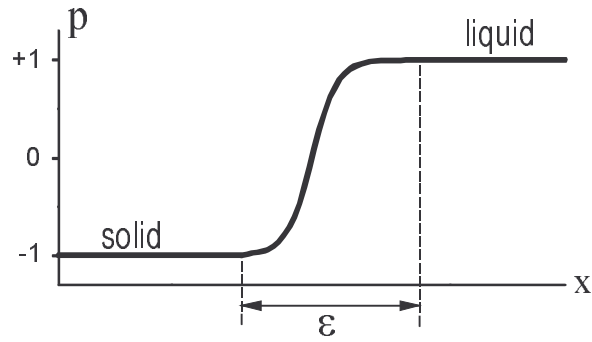


Figure 1 – The order parameter in the PF model describes a diffuse interface between phases, with characteristic length ϵ

Caginalp and Sokolovsky (1991), and Fabbri and Voller (1997) have shown that the use of a suitable large numerical value for ϵ does not compromise the solutions of the PF equations as far as interface progression and temperature histories are concerned (that does, however, introduce a cutoff for short wavelengths which could hinder a selection process in a non-isotropic multidimensional medium).

The system total free-energy F can be written as a first-order expansion in the field p (Landau expansion), and the temperature T :

$$F = \int \left\{ \frac{1}{2} \xi^2 |\nabla p|^2 + f(p, T) \right\} d^3 r \quad (1)$$

In Eq. (1), ξ is a characteristic length of order ϵ . Minimization of the functional F with respect to the order parameter p , followed by a relaxation-time approximation (Fabbri, 1994) with characteristic time α , gives the phase evolution equation

$$\alpha \xi^2 \frac{\partial p}{\partial t} = \xi^2 \nabla^2 p - \frac{\partial f}{\partial p} \quad (2)$$

Solidification (that is, the S-L interface progression) is driven by the potential term $f(p, T)$, which shall have minima at $p = \pm 1$, corresponding to equilibrium solid and liquid states (Fig. 2).

The diffuse interface theory (Allen and Cahn, 1979) relates the surface tension σ to the potential f and to the characteristic length ξ , as follows:

$$\sigma = \sqrt{2} \xi \int_{-1}^{+1} \sqrt{f(p, T)} dp \quad (3)$$

The potential $f(p, T)$ can be chosen by numerical convenience, provided it has the qualitative features depicted in Fig. (2). The detailed form of $f(p, T)$ actually has some impact on the linear behavior of the kinetic parameter, as will become clear later. We follow Kobayashi (1993), and write $f(p, T)$ as a fourth degree polynomial with fixed minima at ± 1 :

$$f(p, T) = \frac{W}{16} \int_{-1}^p (1 - \phi^2)(\phi + m(T)) d\phi \quad (4)$$

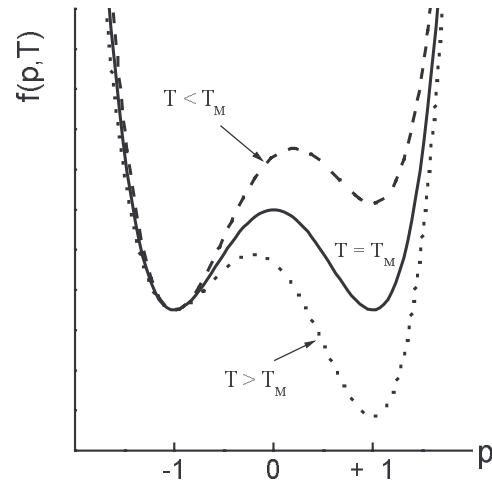


Figure 2 – The phase-field potential, with temperature-dependent local minima. T_M is the equilibrium melting temperature.

W is an arbitrary constant (related to the entropy scale), and the temperature-dependent term $m(T)$ must satisfy $|m(T)| < 1$, in order to have df/dp with three distinct roots. We choose a simple linear form (from here on, we assume $T_M=0$):

$$m(T) = 2\gamma T \quad (5)$$

, restricting γ to a maximum value such that $-1 < m < +1$ for every possible value of temperature the system may exhibit.

2.2 Kinetic relationship for small undercooling

If a travelling wave solution to Eq. (2) is assumed, then $p(x,t) = p(\eta) = p(x-vt)$ satisfies

$$\frac{d^2 p}{d\eta^2} + \alpha v \frac{dp}{d\eta} + \frac{1}{\xi^2} \phi(p, T) = 0 \quad (6)$$

We have written $\phi = \partial f / \partial p$ and v is the local interface velocity. A linear expansion of p in terms of η ($p \sim a\eta$) around the interface region Γ ($p=0$) then gives at once a linear kinetic relation between the local speed and temperature:

$$T_\Gamma = -\frac{8\alpha a \xi^2}{\gamma W} v \quad (7)$$

The constant a in Eq. (7) can be expressed in terms of ξ , and a detailed asymptotic analysis carried out by Karma and Rappel (1996b) gives

$$T_\Gamma = -a_1 \frac{\alpha \xi}{2\gamma} v \quad (8)$$

, where a_1 is a constant of the order unity which depends on the detailed form of the potential $f(p,u)$.

2.3 Thermal transport

Eq. (2) for the phase field must be coupled to a heat transport equation for temperature. A simple model is the usual Fourier law with a source term to account for the latent heat release L at the interface:

$$\rho c \frac{\partial T}{\partial t} + \frac{1}{2} \rho L \frac{\partial p}{\partial t} = K \nabla^2 T \quad (9)$$

ρ , K and c are the medium density, conductivity and specific heat, respectively. Eq. (9) can be given any desired form, including cases when the thermophysical properties vary between phases.

The system of coupled non-linear equations (2) and (9) are then solved over the domain of interest, subjected to the appropriate initial and boundary conditions for the phase and temperature fields. The S-L interface location is determined a posteriori, simply by locating points where the phase variable p crosses zero.

It should be noted that nucleation cannot be taken into account by a mean-field model, such as the Phase-Field free-energy minimization, based on the Landau expansion to the second order, Eq. (1). Being a fluctuation process, nucleation could be simulated within the PF model by introducing noise in the phase evolution equation. Another usual procedure is to specify an initial layer of solid as a starting point for PF simulations.

3. SHARP-INTERFACE LIMIT IN THE TWO-PHASE UNDERCOOLED STEPHAN PROBLEM

Benchmark quantitative tests were intensively made for the PF solutions (Fabbri and Voller, 1995 and 1997, Fabbri, 1994), and they allow confidence in the numerical results for engineering applications.

The overall result shows that excellent agreement between PF simulations and the expected interface progression, field profiles and temperature histories can be attained for a computational value of the interface characteristic length ξ much larger than the actual (microscopic) solid-liquid interface layer. In this respect, a classical solution to a phase-change problem is referred to as the "sharp-interface" limit of the PF model (an excellent recent review on that subject has been provided by Skerka, 2004).

A somewhat stringent test is the solidification from an initially supercooled melt ($T(x,0)=T_{\text{init}}<T_M$, and $T(0,t)=T_s<T_M$ for $t>0$). This gives rise to the so-called "two-phase supercooled Stephan problem", which is classically modeled by imposing an S-L interface at $T=T_M$, that advances through the melt with latent heat release. In this case, heat transport is away from the interface in both directions. It is well known that it is not possible, in more than one dimension, to maintain a flat stable interface in that situation (Kurz and Fisher, 1992). In one-dimensional approximations (slab solidification), there is a similarity analytical solution for semi-infinite domains (Alexiades and Solomon, 1993).

As an illustration (Fabbri, 2000), we consider a 5cm slab of water initially at -10°C but still liquid, impose the fixed temperature -20°C at the left wall ($x=0$), and started solidification at time $t=0$. We show in Fig. (3) the PF numerical results as compared to the similarity solutions after an initial layer of solid was already grown up to $x_0=0.5\text{cm}$. As the analytic solutions are valid for a semi-infinite domain, the boundary temperature at the right-end was kept time-dependent and equal to the value prescribed by the similarity-solution. The pictures also show the numerical PF results for a finite domain, when the right-wall temperature is kept constant at -10°C .

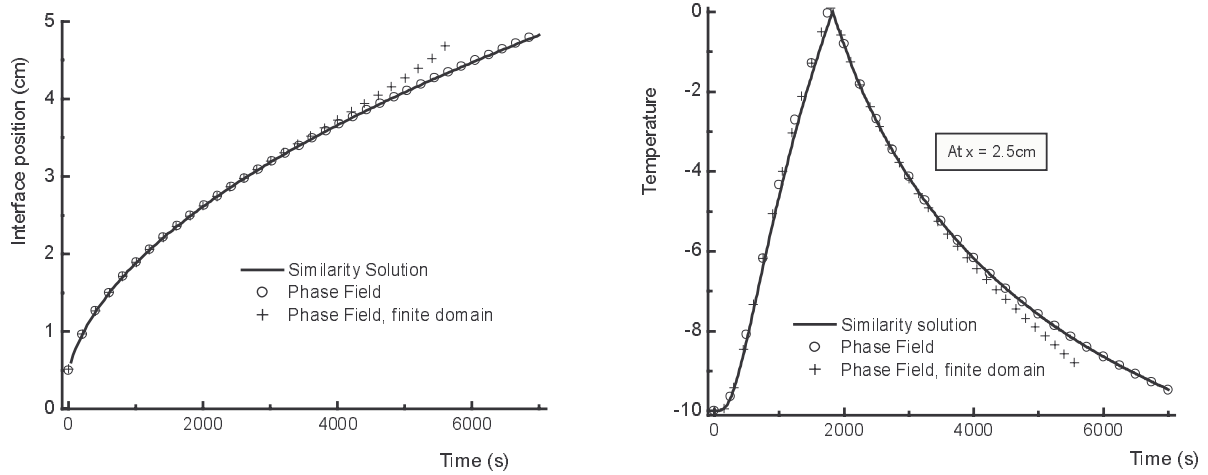


Figure 3 - Comparison between PF calculations and analytic solutions for a model two-phase undercooled Stefan problem

The PF simulation was done over a fixed-grid control-volume discretization with a 500-point mesh. A typical run takes less than half a minute in a 600MHz Pentium III personal computer and a gcc compiler.

4. THERMAL TRANSPORT WITH AN EXTERNAL HEAT SINK

4.1 PF equations

We now consider a one-dimensional (with unit cross-section) slab of a pure material with heat coupling to a thermal sink of known profile $T_\infty(x)$, in which case the PF model reads

$$\begin{cases} \frac{\partial T}{\partial t} + \frac{1}{2} \frac{L}{\rho c} \frac{\partial p}{\partial t} = \frac{K}{\rho c} \frac{\partial^2 T}{\partial x^2} - h(T - T_\infty) & \text{(a)} \\ \alpha \xi^2 \frac{\partial p}{\partial t} = \xi^2 \frac{\partial^2 p}{\partial x^2} + \frac{W}{16} (1 - p^2)(p + 2\gamma T) & \text{(b)} \end{cases} \quad (10)$$

The external heat coupling is described only by an effective heat transfer coefficient h , with corresponding non-dimensional Biot number $Bi = h/\alpha_T$, $\alpha_T = K/(\rho c)$ being the heat diffusivity.

Cases of interest here are when the liquid is kept undercooled ($T \leq T_M$) at all times; if the liquid is at an initial uniform temperature T_0 , the Stefan number is defined as $St = L/c(T_M - T_0)$ and is a dominant parameter for the solid-liquid interface progression.

The PF simulation starts from an initial state where a solid layer is already defined in the region $0 \leq x \leq x_0$. We also take T_∞ constant and uniform, given that the detailed profile of the heat sink is not of concern here. Therefore, for a slab length ℓ , we work with the following initial and boundary conditions:

$$\begin{cases} T(0, t) = T(\ell, t) = T_\infty \\ p(0, t) = -1 \\ p(\ell, t) = +1 \end{cases} \quad \begin{cases} T(x, 0) = T_0 \\ p(x, 0) = \begin{cases} -1 & \text{for } 0 \leq x \leq x_0 \\ +1 & \text{for } x_0 \leq x \leq \ell \end{cases} \end{cases} \quad (11)$$

4.2 Model calibration

The regime $Bi \rightarrow \infty$ can be used to set the potential-dependent constant a_1 in the linear kinetic relationship, Eq. (8). In that limit, we have $T(x,t) = T_0 = T_\infty$ and only Eq. (10b) is to be solved for the S-L interface progression.

For large undercoolings, provision must be made for small deviations of linearity. In practice, kinetic undercoolings at the S-L interface range from very small values (typical of metals, around one Kelvin per meter/second), to a thousand times greater (typical of organic substances, around one Kelvin per millimeter/second). Since non-linear deviations are likely to be strongly potential-dependent, calibration must be done for each specific range.

The Kobayashi potential, Eq. (4), has the advantage of displaying fixed minima at $p = \pm 1$ at all temperatures, provided that the condition $-1 < 2\gamma T < +1$ is met. The actual value of γ affects the form of the double-well potential around those minima, and working too close to the threshold may introduce artificial non-linearities. In this respect, it is convenient to express γ in terms of an entropy scale, defined by the solid-liquid phase change at T_M . Since the entropy S can be obtained from the derivative of the free-energy F with respect to temperature, integration of $\phi(p,T)$ in the interface region, from solid to liquid, gives at once, for the Kobayashi potential,

$$\gamma = \frac{6\Delta S}{W} \quad (12)$$

, where $\Delta S = (S_{\text{liq}} - S_{\text{solid}})$ at T_M .

We found that, for the Kobayashi potential, the smaller the entropy scale, linearity is maintained for higher undercoolings.

We show in Fig. (4) the numeric results of our PF runs for $Bi \rightarrow \infty$ both for small and high kinetic coefficient, for $\Delta S = 0.025$. The model is calibrated by linear fitting over a range of values for the undercooling ΔT . It is seen that, provided the entropy scale is given a small enough value, kinetic non-linear deviations in the Kobayashi model are very weak and can be disregarded for most applications.

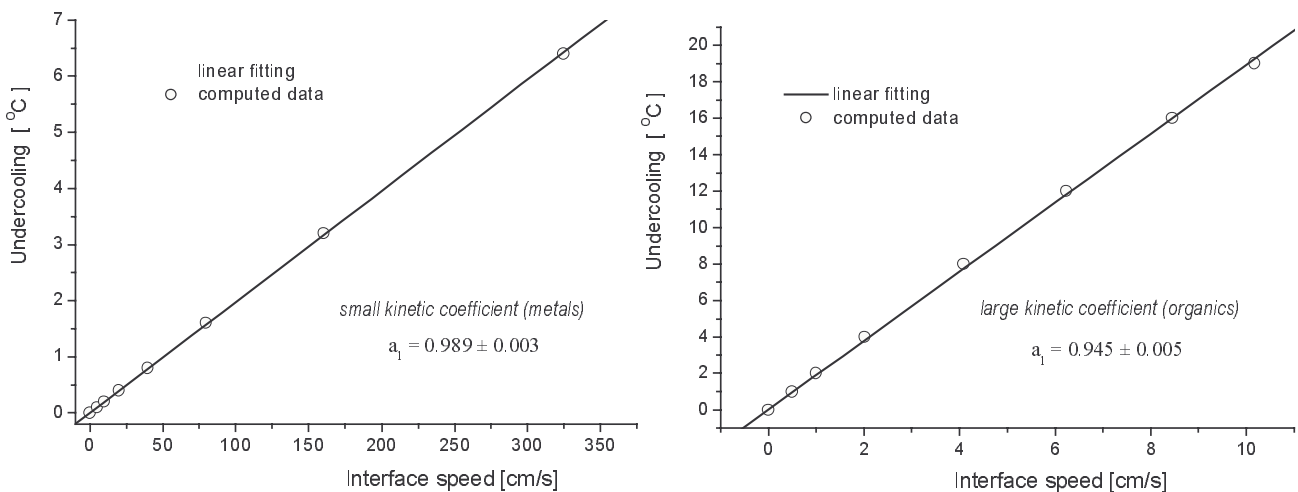


Figure 4 - Linear fitting the form parameter a_1 for the linear kinetic relationship in the PF-Kobayashi model.

Details of the PF computation are as follows: Eq. (10b) is discretized over a fixed-control-volume grid, totally-implicit in time. The tridiagonal non-linear system of equations is solved iteratively by a local-source linearization scheme. An $N=500$ uniform mesh cover the x-domain $[0, \ell]$, such that $\Delta x = \ell/N$, and the time interval Δt is chosen as large as possible as far as convergence is obtained. The slab length is $\ell=5\text{cm}$, the interface length parameter $\xi = 1.25\Delta x$, and $W=8.0$. Those PF settings were the same as the ones employed in the simulation of the two-phase undercooled Stephan problem described above in Section 3.

5. PF RESULTS FOR FINITE BIOT VALUES

The interface progression and temperature, as well as a typical temperature history were computed for values of Bi ranging from 0 (pure conduction inside the material) to ∞ (fixed uniform temperature, as described in the preceding Section). We set the material parameters as $K=c=\rho=L=1$ ($St=1.0$), and the domain is initially at $T_0=0.0$.

We see in Fig. (5) the computed interface progression, both for small ($\alpha=0.06$, corresponding to 2.0 Kelvin per meter/second) and large ($\alpha=6.0$, corresponding to 2.0 Kelvin per centimeter/second) kinetic coefficients. The (fixed) temperatures of the heat sink were $T_\infty = -0.10$ and -12.0 , respectively.

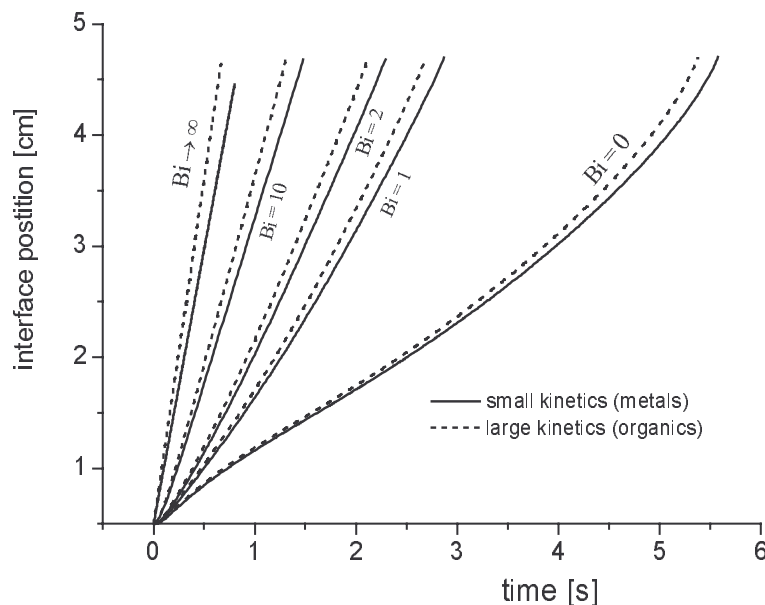


Figure 5 - Interface progression as computed by the PF model for a range of Biot numbers.

We note that there were no qualitative differences between the results for small and large kinetics, so we display in Fig. (6) and (7) the interface temperature and history at $x=2.5$ only for the small kinetic case.

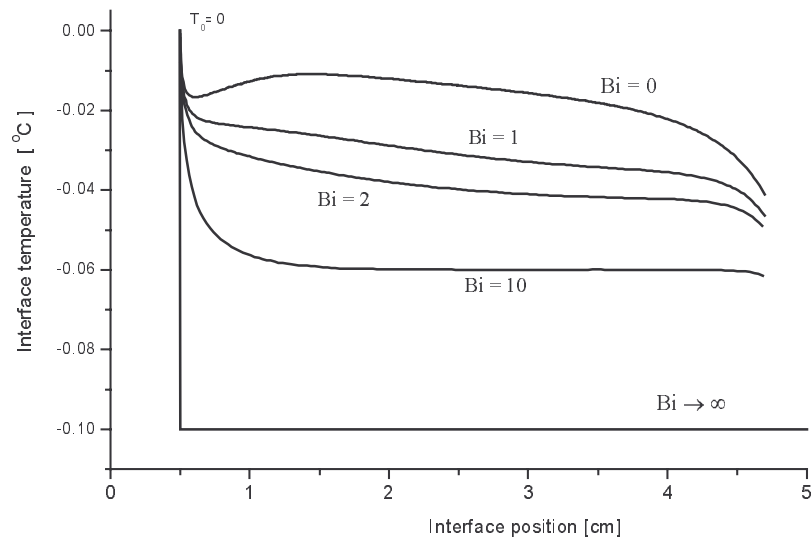


Figure 6 - Temperature at S-L interface as computed by the PF model.

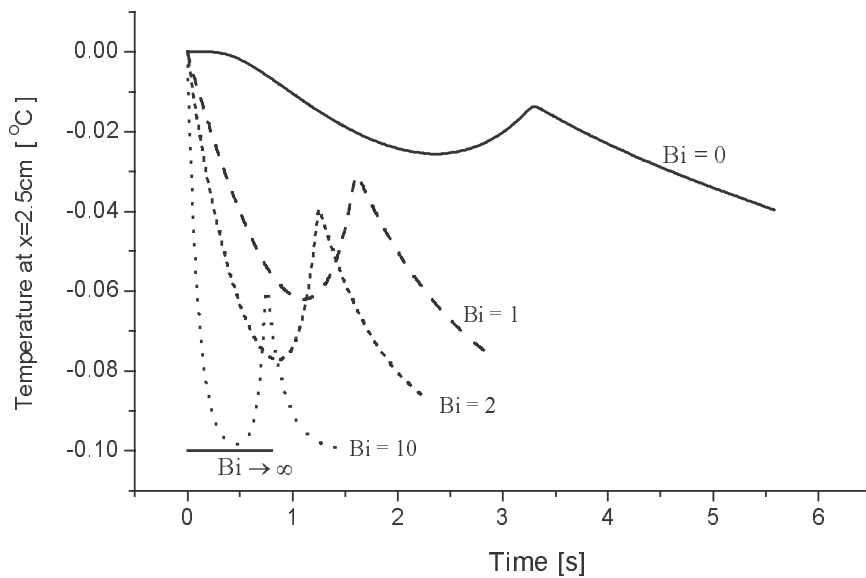


Figure 7 - PF results for the temperature history at location $x=2.5\text{cm}$.

It is worth noting in Fig. (7) the sharp raising of the local temperature during the passage of the interface, which becomes sharper with increasing values of the Biot number.

All simulations were done in a 650MHz Pentium III personal computer with a gcc compiler, and a typical run takes less than half a minute.

6. CONCLUSIONS AND COMMENTS

We have described a simple numerical procedure to match the kinetic parameters of the phase-field technique to the actual material properties. Our numerical simulations show that, for the Kobayashi potential, the form factor that appears in Karma and Rappel's analysis is indeed very close to unity.

As an illustration, we have worked out some simple examples of PF simulation in the presence of high undercooling, and those are to be compared to classical models, where the interface kinetics are treated *ad hoc*. In PF models, the underlying physics is treated in a very natural manner, and metastable states require no additional assumptions.

This work is a first step towards applying PF methods for laser-assisted rapid solidification, where solidification rates approach the diffusive atomic velocity at the interface, and therefore large deviations from local equilibrium are expected.

The predicted linear relation between front speed and temperature for low undercoolings is an essential feature of the PF equations, and non-linear effects for very high front speeds are potential-dependent. In that respect, more research is needed in order to model PF potentials directly from the material thermodynamics (constitutive equations), which could explain the variety of observed material-dependent experimental behavior.

It should be noted that distinct PF models can be tailored which exhibit essential non-linear kinetic behavior (Fazenda, Travelho and Fabbri, 1996); that can be done either by a non-linear temperature dependence of the potential or by adopting a non-linear relaxation towards equilibrium. Also, in two or three-dimensional simulations, the interfacial kinetics can be made anisotropic, which is suitable to treat, e.g., faceted crystal growth (Uehara and Skerka, 2003).

Recently, kinetic-dominated models were reported for the study of morphological transitions at high undercoolings. The usual formulations of the PF model, for those purposes, require an interface length of the order of the capillary length, and are very computationally expensive. A modification of the PF potential which allows computation for an interface thickness many times greater than the capillary length was recently proposed by Vestigian and Goldenfeld (2003).

REFERENCES

- Allen, S.M. and Cahn, J.W., 1979. A Microscopic Theory for Antiphase Boundary Motion and its Application to Antiphase Domain Coarsening. *Acta Metall.* **27**, pp.1085-1095.
- Alexiades, V. and Solomon, A.D., 1993. *Mathematical Modeling of Melting and Freezing Processes*, Hemisphere, Washington.
- Braun, R.J., McFadden, G.B. and Coriell, S.R., 1994. Morphological instability in phase-field models of solidification. *Phys.Rev.* **E49**(5), pp.4336-4352.
- Caginalp, G., 1980. An Analysis of a Phase Field Model of a Free Boundary. *Arch. for Rat. Mech. Anal.* **92**(3), pp.205-245.
- Caginalp, G. and Socolovsky, E.A., 1991. Computation of Sharp Phase Boundaries by Spreading: The Planar and Spherical Symmetric Cases. *J.Comp.Phys.* **95**, pp.85-100.
- Fabbri, M., 1994. The Phase-Field Method in Engineering: Behavior Under Various Solidification Regimes. *Proceedings of the 5th Thermal Sciences Brazilian Meeting*, São Paulo, SP, Brazil, pp. 329-333.
- Fabbri, M. and Voller, V.R., 1995. Numerical Solution of Plane-Front Solidification with Kinetic Undercooling. *Num.Heat Transf.* **27**(4), pp.467-486.

- Fabbri, M. and Voller, V.R., 1997. The Phase-Field Method in the Sharp-Interface Limit: A Comparison between Model Potentials. *J.Comp.Phys.* **130**, pp.256-265.
- Fabbri, M., 2000. Phase-Field Solutions for the Classic One-Dimensional Two-Phase Supercooled Solidification Problem. *Projeções* **18** (EDUSF, Bragança Paulista, SP, Brasil, ISSN 0103-7757), pp.11-20.
- Fazenda, A.L.; Trivelho, J.S. and Fabbri, M., 1996. Modeling Kinetic Undercooling through Phase-Field Equations with Non-Linear Dynamics. *Proceedings of the 6th Thermal Sciences Brazilian Meeting*, Florianópolis, , SC, Brazil, pp. 953-956.
- Karma, A. and Rappel, W.-J., 1996a. Numerical Simulation of Three-dimensional Dendritic Growth. *Phys. Rev. Lett.* **77**, pp.4050-4053.
- Karma, A. and Rappel, W.-J., 1996b. Phase-field method for computationally efficient modeling of solidification with arbitrary interface kinetics. *Phys. Rev. E* **53**, R3017-3020.
- Kobayashi, R., 1993. Modeling and Numerical Simulations of Dendritic Crystal Growth. *Physica D* **63**, pp.410-423, 1993.
- Kurz, W. and Fisher, 1992. *Fundamentals of Solidification*, Trans-Tech Publications, Switzerland.
- Lan, C.W.; Shih, C.J. and Hsu, W.T., 2004. Long-time scale morphological dynamics near the onset of instability during directional solidification of an alloy. *J. Crystal Growth* **264**, pp. 379–384
- Skerka, R.F., 2004. Morphology: from sharp interface to phase field models. *J. Crystal Growth* **264**, pp.530–540.
- Uehara, T. and Skerka, R.F., 2003. Phase field simulations of faceted growth for strong anisotropy of kinetic coefficient. *J. Crystal Growth* **254**, pp.251–261.
- Vetsigian, K. and Goldenfeld, N., 2003. Computationally efficient phase-field models with interface kinetics. *Phys. Rev. E* **68**, pp.0606011-4(R).
- Warren, J.A., 1995. How Does a Metal Freeze? A Phase-Field Model of Alloy Solidification. *IEEE Comp.Sci.Eng.* **2**(2), pp.39-49.